Observation of Shock Transverse Waves in Elastic Media

S. Catheline, J.-L. Gennisson, M. Tanter, and M. Fink

Laboratoire Ondes et Acoustique, ESPCI, Université Paris VII, U.R.A. CNRS 1503, 10 rue Vauquelin, 75231 Paris Cedex 05, France

(Received 24 September 2002; published 14 October 2003)

We report the first experimental observation of a shock transverse wave propagating in an elastic medium. This observation was possible because the propagation medium, a soft solid, allows one to reach a very high Mach number. In this extreme configuration, the shock formation is observed over a distance of less than a few wavelengths, thanks to a prototype of an ultrafast scanner (that acquires 5000 frames per second). A comparison of these new experimental data with theoretical predictions, based on a modified Burger's equation, shows good agreement.

DOI: 10.1103/PhysRevLett.91.164301 PACS numbers: 43.25.+y, 43.35.+d, 43.80.+p

Although the nonlinear behavior of transverse waves is common to optics (electromagnetic field in a nonlinear isotropic dielectric), seismology, and acoustics, no direct experimental observation of a shock transverse wave has been made up to now. As a comparison the nonlinear behavior of longitudinal waves in fluids or solids is well established from a theoretical and an experimental point of view [1], and the sawtooth shape of a shock longitudinal wave is a well-known result. Now, the shape of a shock transverse wave is quite unknown though it has been theoretically predicted [2–4]. The main reason for this lack of experiment is that nonlinear effects of transverse waves are very small. For example, in acoustics, they are 1 order of magnitude smaller than the nonlinear effects of longitudinal waves. Moreover, the high stiffness of crystal or metal does not allow any source to impose a high particle velocity compared to the speed of the wave itself, and a typical Mach number in such media is 10^{-4}. In the field of soft solids, such as biological tissues (muscle, fat, and breast) or Agar-gelatin based phantom (a soft tissue model), the very low value of the shear elasticity (typically 2.5 kPa) allows the propagation of a low frequency transverse wave (100 Hz) with a very high particle velocity (0.6 $\mathrm{m\,s^{-1}}$) compared to its speed (1.6 $\mathrm{m\,s^{-1}}$). Thus Mach numbers as large as unity are obtained. Consequently, in this peculiar configuration, third order nonlinear effects become very high and clearly modify the transverse wave shape.

In this Letter, we present an experimental study of a shock transverse wave by using a novel ultrafast ultrasonic scanner. It provides images of the tissues similar to a standard echographic device but with a rate of 5000 frames per second (200 times higher than a conventional scanner). This ultrafast scanner (Fig. 1) was developed in our laboratory to observe low frequency shear waves in the body. It includes a medical ultrasonic array (5 MHz) with 128 channels [5]. Each channel is connected to a large memory (2 Mbytes), and the echoes are sampled at 50 MHz and digitized with 9 bit resolution. In a typical experiment, 250 echographic images (at a 3000 Hz frame rate) are recorded in memory. A displacement movie is obtained using cross correlation algorithms between successive speckle images [6]. Indeed, the Agar powder (3%) in suspension in a solid gelatin solution (3%) gives birth to backscattered ultrasonic signals (the speckle). Tracking methods such as cross correlation algorithms allow one to interpret the speckle modifications induced by low frequency shear waves in terms of tissue motion within the medium. This apparatus can detect displacement as small as 1 μm. The whole technique is known as transient elastography. As shown in Fig. 1, the low frequency (100 Hz) shear wave is generated by shaking transversally a rigid aluminum plate (11 × 17 cm) applied on one side of the phantom with a vibrator (Bruel&Kjaer 4809 type). The transverse displacement field of the shear wave is measured in one dimension along the axis of the rigid plate on a distance of 40 mm

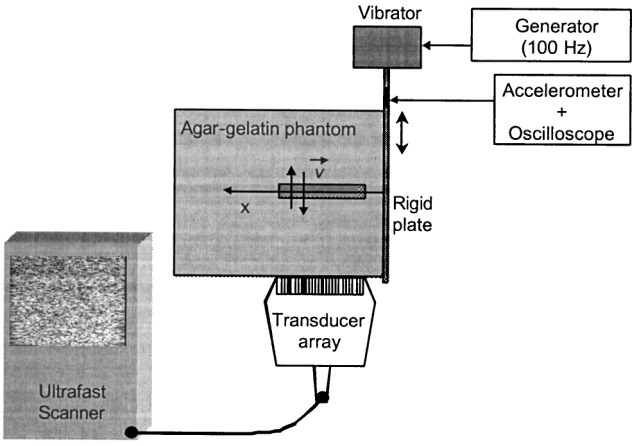

FIG. 1. Experimental setup. Transient elastography technique: a medical transducer array connected to an ultrafast scanner insonifies a tissue-mimicking phantom. A 100 Hz shear wave train is generated by a vibrator from a rigid plate applied on one side of the phantom. Simultaneously, frames (at a 3000 Hz repetition rate) are stored in memory. With cross correlation algorithms between frames, the transverse displacement field (along the z axis) of the shear wave is measured along the central axis of the plate (parallel to the x axis).

 0031-9007/03/91(16)/164301(4)$20.00

which represents a few shear wavelengths. An accelerometer is set on the vibrator to control the possible harmonics of the source itself.

The detailed development of the elastic nonlinear theory can be found in numerous textbooks [7]. Here we summarize the general equations. For a transverse wave, it is well established that for symmetry reasons, the quadratic terms vanish in the stress-strain relationship which implies that nonlinear effects are one order smaller than for the longitudinal wave. Developed to the third order, the stress-strain relationship can be expressed as

$$\sigma = E\varepsilon + \gamma\varepsilon^3 - \eta\frac{\partial\varepsilon}{\partial t}, \tag{1}$$

where σ, ε designate the stress and the strain, respectively. E, γ are, respectively, the second and fourth order elastic moduli. In the Newtonian viscous term on the right-hand side of Eq. (1), η stands for the viscous coefficient. By inserting (1) into the equation of motion and by using the relation $\partial/\partial t = -c_o(\partial/\partial x)$, we get the one wave equation for the particle velocity v:

$$\frac{\partial^2 v}{\partial x^2} - \frac{\rho_o}{E}\frac{\partial^2 v}{\partial t^2} = -\frac{3\gamma}{c_o^2 E}\frac{\partial}{\partial x}\left(v^2\frac{\partial v}{\partial x}\right) + \frac{\eta}{E}\frac{\partial^3 v}{\partial t\partial x^2}, \tag{2}$$

where ρ_o is the density and $c_o = (E/\rho_o)^{1/2}$ is the speed of a small amplitude wave. Then, moving to variables $y = t - x/c_o$, $x' = x$ in order to observe the wave shape in the referential moving at the speed c_o and assuming the dependence on x to be slow, one can readily obtain as the evolution equation the modified Burgers equation:

$$\frac{\partial v}{\partial x} - \frac{3\gamma}{2\rho c_o^5}v^2\frac{\partial v}{\partial y} = \frac{\eta}{2\rho c_o^3}\frac{\partial^2 v}{\partial y^2}. \tag{3}$$

In the simple case of weak viscosity, the modified Burgers equation has the following Riemann solution:

$$v = f(y + \alpha v^2 x), \tag{4}$$

where f is an arbitrary waveform function defined by the boundary condition $v(0, t) = f(t)$ and $\alpha = 3\gamma/2\rho c_o^5$. Then the local propagation speed equals

$$c = c_o(1 + c_o\alpha v^2). \tag{5}$$

Using the sinusoidal boundary condition, the shock distance or the discontinuity distance can be deduced from Eq. (4):

$$L_S = (\alpha\omega v_o^2)^{-1}, \tag{6}$$

where ω stands for the angular frequency of the shear wave.

A finite-difference simulation based on the McDonald and Ambrosiano algorithm was used to compute the Burgers equation with viscosity [8]. It consists of a hybrid upwind scheme. A high order flux correction method which is a numeric "equal areas rule" following from the Rankine-Hugoniot relations [9] avoids the numerical instability. Consequently, in the simulation, the flux correction algorithm computes the extraabsorption occurring from the shock distance due to high gradients, whereas the viscous absorption due to the propagation through a dissipative medium is taken into account by the classical Newtonian viscous term in (1).

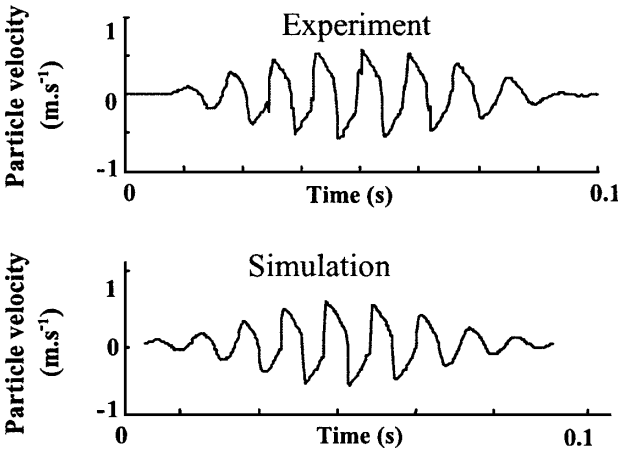

FIG. 2. Comparison between the experimental and theoretical particle velocities as a function of time measured at a point located 15 mm away from the source. The central frequency of the emitted signal is 100 Hz.

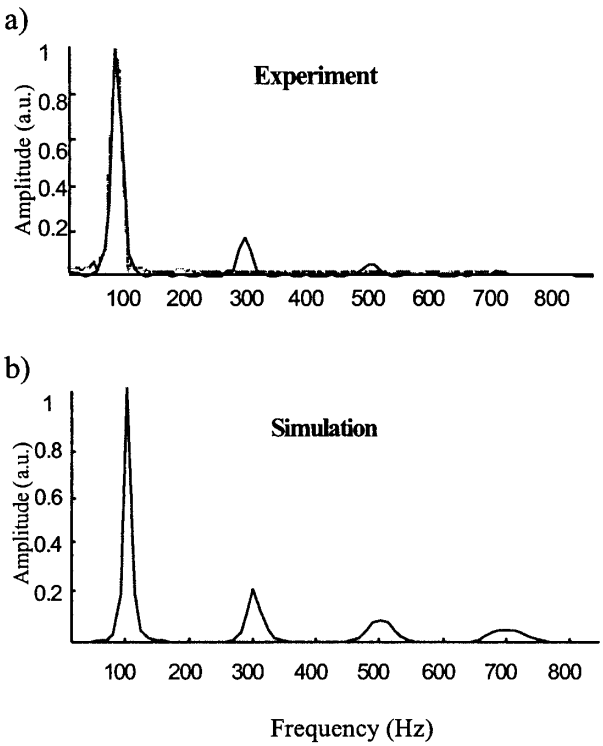

FIG. 3. (a) Normalized experimental spectrum of the acceleration signal measured on the source (dashed line) and of the particle velocity at a point located at 15 mm away from the source (solid line). (b) As predicted by theory, only odd harmonics appear on this spectrum.

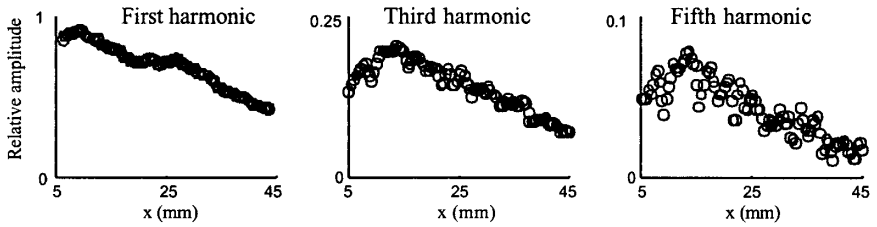

FIG. 4. Experimental amplitude of each harmonics as a function of the propagation distance x. A part of the energy of the first harmonic is transmitted to higher harmonics.

Indeed, the relative importance of nonlinearity and viscous dissipation is characterized by the dimensionless Gol'dberg number $N_G = L_A/L_S$ defined as the ratio of the attenuation length to the shock distance. The attenuation length (the inverse of the attenuation coefficient) is obtained experimentally by measuring the decreasing law of a small amplitude shear wave: $L_A = 57$ mm. Therefore, the Gol'dberg number for each decreasing source amplitude is 8.6, 6.9, 5.5, and 4.2. Given that viscous dissipation dominates for small values of N_G, it clearly appears that the viscous phenomenon has to be taken into account in the numerical simulation. The viscous coefficient used in the simulation (0.4 Pa s) is deduced from the measurements of both the speed (1.6 m s^{-1}) and the attenuation length.

To summarize, the simulation parameters, chosen as close as possible as in the experiment are 100 Hz, 0.6 m s^{-1}, 1100 kg m^{-3}, 1.6 m s^{-1}, 3000 Hz, 5.1 kPa, and 0.4 Pa s for the shear wave frequency, the source particle velocity, the density, the shear wave speed, the sampling frequency, the fourth order moduli, and the viscous coefficient, respectively. Very good agreement is found between the experiment and the simulation (Fig. 2). The temporal shape of the particle velocity at 15 mm away from the source is not a sawtooth shape as for the longitudinal waves. From a theoretical point of view, this result is well explained considering the local speed [Eq. (5)]. Each point of the wave profile travels with its own constant speed, which depends on the value of the square of the particle velocity v^2. As a result and contrary to the longitudinal wave, the high amplitude parts of the wave travel faster whatever the sign of the particle velocity: the slope steepens simultaneously on the positive and the negative half period. This can be interpreted as a consequence of the symmetric behavior of the displacement field as regard to the propagation direction. As predicted by theory, for such a wave one can observe only odd harmonics at 100, 300, 500, and 700 Hz (Fig. 3). As a comparison, the spectrum of the accelerometer set on the vibrator (the shear wave source) contains only the fundamental harmonic at 100 Hz.

The amplitude evolutions of the first, the third, and the fifth harmonics as functions of propagation distance (or depth within the medium) are represented in Fig. 4. The first harmonic decreases because the medium is not lossless as is shown in the next part and also because the nonlinear phenomenon transmits a part of the energy to higher harmonics. Indeed, the amplitude of the third and the fifth harmonics grows until dissipation effects become predominant (12.5 mm). The experimental amplitudes of the third harmonic as a function of depth for

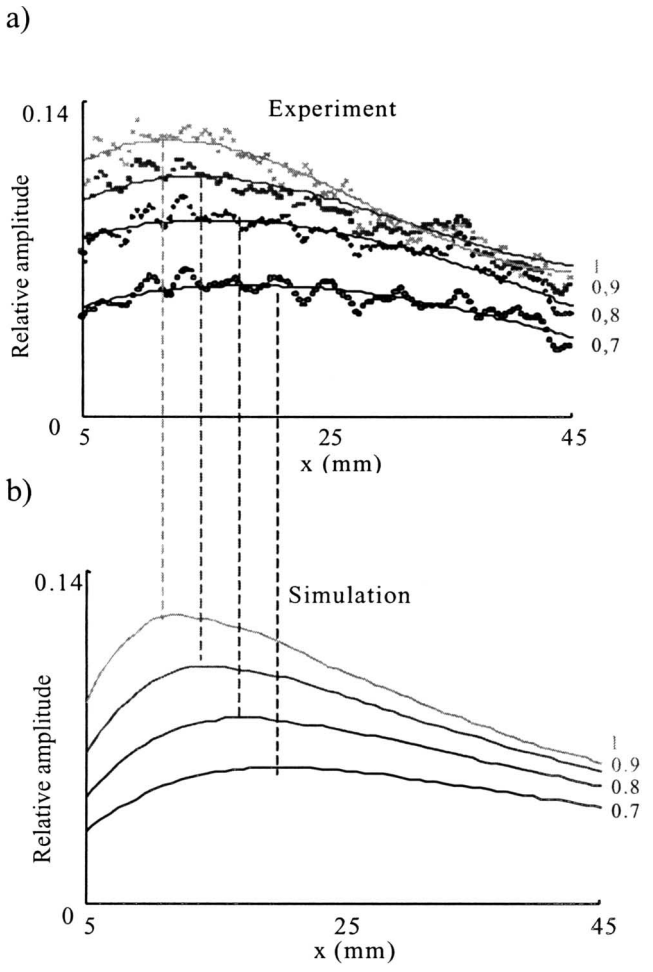

FIG. 5. Amplitude of the third harmonic as a function of propagation distance x. Each curve from the top corresponds to a decreasing emitted signal (from 1 to 0.7). In the experiment (a) and in the simulation (b), the maximum is moving away from the source as the source amplitude decreases. A 3% agreement on the maximum positions is found between experiment and simulation.

source amplitudes in arbitrary units ranging from 1 to 0.7 are shown in Fig. 5(a). A third order polynomial fit on the experimental measurements allows one to estimate the positions of the four maxima for each emitted amplitude. These positions are 12.5 mm, 14.2 mm, 16.9 mm, 20.1 mm, respectively. Thus the amplitude maximum of the third harmonic is reached further away from the source as the emitted amplitude decreases. This illustrates the well-known result according to which the shock distance increases when the wave amplitude decreases. In Fig. 5(b), the simulated amplitude of the third harmonic as a function of propagation distance shows the same general shape as in the experiment. The positions of the maxima for each emitted amplitude are 12.6, 14.6, 17.2, and 20.5 mm which is in agreement within 3% with the experiments.

In conclusion, we have proposed the first direct experimental observation of a shock transverse wave in solids. In particular, we have emphasized that studying the propagation of elastic waves in soft solids is a fruitful way to revisit the nonlinear wave theory and to bring new experimental validations in this field.

The authors express their grateful thanks to P. Rasolofosaon, J.-L. Thomas, C. Barrière, O. Bou Matar, and V. Gusev for useful discussions.

[1] J. S. Mendousse, J. Acoust. Soc. Am. **25**, 51 (1953).
[2] R. W. Lardner, J. Elast. **15**, 53 (1985).
[3] E. A. Zabolotskaya, Sov. Phys. Acoust. **32**, 296 (1986).
[4] I. P. Lee-Bapty and D. G. Crighton, Philos. Trans. R. Soc. London A **323**, 173 (1987).
[5] L. Sandrin, M. Tanter, S. Catheline, and M. Fink, IEEE Trans. Ultrason. Ferroelectr. Freq. Control **49**, 425 (2002).
[6] J. Ophir, I. Céspedes, H. Ponnekanti, Y. Yasdi, and X. Li, Ultrasonic Imaging **13**, 111 (1991).
[7] K. Naugolnykh and L. Ostrovsky, *Nonlinear Wave Processes in Acoustics* (Cambridge University Press, New York, 1998), p. 74.
[8] B. E. McDonald and J. Ambrosiano, J. Comput. Phys. **56**, 461 (1984).
[9] L. Landau and E. Lifshitz, *Hydrodynamics* (Mir, Moscow, 1986), p. 536.